Tidal Steam Turbine Blade Fault Diagnosis Using Time-Frequency Analyses.

Matthew Allmark[1], Paul Prickett[2], Roger Grosvenor[3], Carwyn Frost[4]

Cardiff Marine Energy Research Group (CMERG), Cardiff School of Engineering,
Cardiff University, Wales.

[1]allmarkmj1@cardiff.ac.uk

[2]prickett@cardiff.ac.uk

[3]grosvenor@cardiff.ac.uk

[4]frostC1@cardiff.ac.uk

Abstract— **Tidal Stream Turbines are developing renewable energy devices, for which proof of concept commercial devices are been deployed. The optimisation of such devices is supported by research activities. Operation within selected marine environments will lead to extreme dynamic loading and other problems. Further, such environments emphasise the need for condition monitoring and prognostics to support difficult maintenance activities.**

This paper considers flow and structural simulation research and condition monitoring evaluations. In particular, reduced turbine blade functionality will result in reduced energy production, long down times and potential damage to other critical turbine sub-assemblies. Local sea conditions and cyclic tidal variations along with shorter timescale dynamic fluctuations lead to the consideration of time-frequency methods.

This paper initially reports on simulation and scale-model experimental testing of blade-structure interactions observed in the total axial thrust signal. The assessment is then extended to monitoring turbine blade and rotor condition, via drive shaft torque measurements. Parametric models are utilised and reported and a motor-drive train-generator test rig is described. The parametric models allow the generation of realistic time series used to drive this test rig and hence to evaluate the applicability of various time-frequency algorithms to the diagnosis of blade faults.

Keywords — Condition Monitoring, tidal stream turbine, Time-Frequency Methods, Rotor Fault Diagnosis, motor – generator test rig.

I. INTRODUCTION

Research within the Cardiff Marine Energy Research Group (CMERG) has established a series of generic design guidelines [1] for the developing commercial deployment of Tidal Stream Turbines (TST). The mathematical models combine Computational Fluid Dynamics (CFD) and structural Finite Element Analysis (FEA) to provide Fluid-Structure-Interaction (FSI) results. Within a structured framework of simulations, the overall aim is to produce non-dimensionalised power and thrust curves [2], along with flow visualisations, for a variety of configurations and realistic flow conditions.

The modeling studies considered relate specifically to Tidal Stream Turbines rather than any other tidal or wave devices. Many such devices have horizontal axis configurations, and it is such Horizontal Axis Tidal Turbines (HATT) that are considered. Fig. 1. [3] shows the general arrangement for a HATT installation and summarises the main parameters and effects of interest.
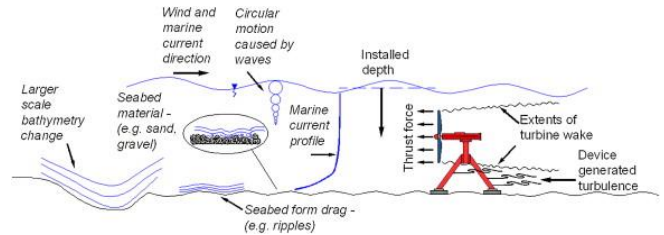

Fig. 1. Horizontal Axis Tidal Turbine (HATT) [3]

The overall modeling studies are briefly reviewed in section II. Previous studies [4] had compared results for designs with varying numbers of blades and had confirmed the optimum blade angle setting for a 3-blade option. Section III introduces condition monitoring considerations and summarises the components of experimental validation testing that relate to time-frequency analysis of total axial thrust measurements. Such results were for flume based testing with plug flow profiles. Recent studies [5] have used profiled flow conditions and with the addition of surface waves in attempts to provide more realistic flow conditions. Section IV compares the experimental axial thrust results, for both optimum blade settings and with a deliberately non-optimum blade setting, to more specific simulation studies. The non-optimum blade setting, with an offset pitch angle, was used to represent a lumped-parameter representation of fault conditions for one of the 3 blades. Section IV also discusses the development of parametric models for the axial thrust considerations. These were developed to improve on the monitoring results, in light of the legacy dataset limitations, and to avoid the relatively long run times for the increasingly complex FSI simulation models. Section V details the

complimentary new studies into parametric modeling of drive shaft torques for dynamic and realistic flow conditions. These are tested via a motor-driveshaft-generator test rig, which is also described in Section V. Example results and an assessment of time-frequency processing methods and their applicability are provided in Section VI. The paper finishes with a discussion of the proposed methods and conclusions on the potential of both suitably processed axial thrust and drive shaft torques as constituents of future TST condition monitoring systems.

II. MATHEMATICAL MODELLING

Within CMERG the CFD / FEA / FSI simulation models for horizontal axis tidal turbines (HATT) have been considered in a non-dimensionalised manner and have led to generic power and thrust performance curves for use by designers.

The performance charts generated by the modeling activities include a non-dimensionalised power curve. Also of interest, for the initial condition monitoring evaluations, is a non-dimensionalised axial thrust curve. Fig. 2. [2] is an example of a power curve, plotted as power coefficient, C_p vs tip speed ratio, TSR. C_p is the power coefficient and is the ratio of the actual power produced to the theoretical fluid dynamic power, this being proportional to the flow velocity cubed. The tip speed ratio (TSR) is a non-dimensional measure of the angular velocity of the HATT. Figure 2 shows the modeling results for a 0.5 m diameter, 3 blade turbine subjected to a plug flow of 1 $m.s^{-1}$. Superimposed, with appropriate error analysis bars are the matching experimental results. An accepted consideration is the variation of flow velocity with the depth of water for a selected installation site. The 2 main approaches have been to assume (i) plug flow, where the flow velocity is constant and (ii) a power law profile. Simulation and experimental work is on-going to provide results for realistic installation conditions. In this paper the experimental axial thrust results are for plug flow tests. The parametric modeling of drive torques includes provision for effects in addition to simple plug flow.
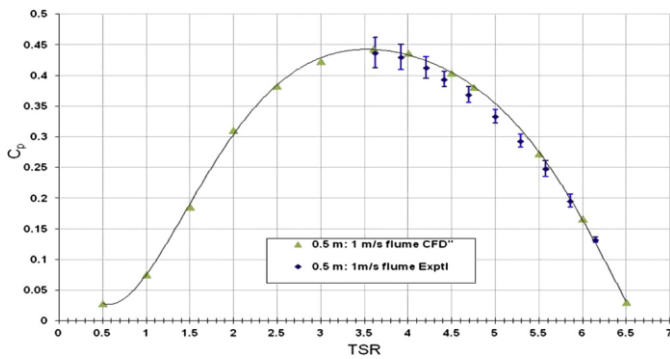
Fig. 2. Power curve for 0.5m diameter turbine with plug flow [2]

Fig. 3. [2] shows the non-dimensional axial thrust curve from the same modelling exercise, plotted as thrust coefficient, C_T vs tip speed ratio, TSR. C_T is the thrust coefficient and is the ratio of the actual thrust produced to the theoretical fluid dynamic thrust, this being proportional to the flow velocity squared.
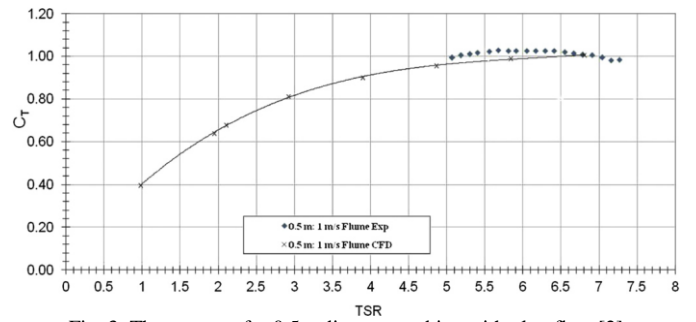
Fig. 3. Thrust curve for 0.5m diameter turbine with plug flow [2]

As stated, the CFD models have been extended to include Fluid-Structure Interactions (FSI) [5]. The experimental testing has also been developed to allow profiled flow testing, in addition to the original plug flow testing. The addition of surface waves has also been developed at the water flume facility at Liverpool University. These aspects are not considered for the experimental axial thrust dataset considered in this paper.

III. CONDITION MONITORING AND PROGNOSTICS

Condition monitoring and fault diagnosis is considered to be elemental in developing marine current turbine energy extraction [6]. Tidal energy technology has yet to be proven with regard to long term operational availability and reliability. It is accepted that the harsh marine environments and problems with accessibility for maintenance may exasperate availability and reliability problems. Minimising uncertainty surrounding the operation and maintenance of such devices will thus be crucial in improving investor confidence and achieving economically viable power extraction [7].

In many cases the proposed monitoring schemes are deemed to be analogous to those deployed on wind turbines [8]. The operating conditions and medium are however vastly different.

Investigations within CMERG, reported in more detail elsewhere [9], began with consideration of a subset of the monitoring system, namely the use of supporting structure based sensors. The support structure sensors are simpler to install and interface to. Analysis of the axial thrust signals identified some low-level cyclic background variations, with these being correlated to the interactions between the rotating blades and the supporting structure. The potential for frequency domain and time-frequency analysis methods were considered and reported.

In this paper the monitoring of blade faults is developed. The blades of Tidal Stream Turbines (TST) are significant in initial turbine costs and are vital to the on-going economic power extraction once the TSTs are installed. Operation within the marine environment will mean that turbine blades are subjected to extreme loading, varying loads and biofouling; as well as being at risk of cavitation. The loss of functionality of a turbine blade will result in reduced energy delivery, long downtimes and if undetected could lead to damage of other critical turbine sub-assemblies. There are significant challenges to overcome if at site turbine maintenance is to be performed. Condition monitoring and associated prognostic methods will provide invaluable information for the required logistical efforts.

Recent research advances have been reported [10][11], that show the potential of using turbine drive shaft torque measurements for monitoring purposes. The turbine drive shaft torque can be measured easily via the power output from the

turbine generator. If is successfully implemented it would negate the need for sensors mounted directly on the turbine rotor. This may be of specific interest to TST developers as such rotor-mounted sensors are likely to face reliability issues due to the harsh marine environment. In order to fully realise such a monitoring approach significant research is required to develop associated signal processing methods and to develop an understanding of the reliability of such an approach under stochastic sea conditions. This paper seeks to inform both of the above through stochastic turbine simulations and appraisal of time-frequency signal processing approaches. These are reported in section V. The prior availability and analysis of the axial thrust results enabled the establishment of this approach. These results, as stated above, are summarised in the following section.

IV MONITORING OF TOTAL AXIAL THRUST

A series of scale model turbines have been developed by the CMERG group for water flume testing. The experimental testing is reported in more detail elsewhere [12]. For this paper a summary of the experimental testing is provided, and concentrates on the results obtained from axial thrust measurements.

For the appropriate tests a 0.5 m diameter, 3 blade turbine was used. Each blade pitch angle was adjustable and from previous testing the optimum blade pitch angle had been determined to be 6° for the configuration in use. This prior testing information was also utilized to simulate a blade fault. In this case one of the blades was deliberately offset, to a pitch angle of 15°.

The water flume was configured and operated to provide plug flow conditions (constant flow with water depth) and an average axial flow velocity of 0.94 m.s^{-1}.

Fig. 4. shows the general setup for the water flume tests. The junction between the vertical turbine support tube and the horizontal supporting frame was fitted with a force block. The strain gauge arrangement of the force block enabled the measurement of the total axial thrust.

Water depth (a) = 0.85 m
Depth to turbine rotation axis (b) = 0.425 m
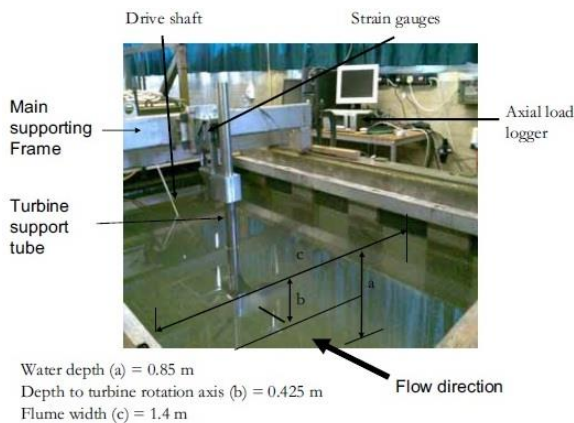Flume width (c) = 1.4 m

Fig. 4. Liverpool University Water Flume and Experimental Setup.

A direct drive servo motor was used to generate controllable torques in opposition to those from the flow and turbine blades. Test results were obtained for a range of conditions from within the turbine performance curve. These ranged from the peak power conditions down to the free-wheeling condition with negligible power output. The integral servo motor used to oppose

and control the generated motion was capable of delivering a maximum torque of approximately 4.92 Nm. The individual results are classified by a percentage torque index with ranging from 45% (peak power) down to 0% (free- wheeling).

Each test typically ran for between 90 and 150 s. and in total 3 signals were recorded: the servo motor current (used to calculate power outputs); the angular velocity of the turbine; and the total axial thrust. Companion results were obtained for 'optimum' blades and 'offset' blade representing normal and single blade faults respectively. The blade fault at the peak power setting, for example, manifested itself as reduced power generation (power coefficient C_p reducing from 0.43 to 0.37 as a typical result) and reduced angular velocity (TSR reducing from 4.2 to 3.7 as typical result).

Of more relevance to the current discussion, the experimental non-dimensional thrust curve, for the range of conditions tested, is shown in Fig. 5. The effect of a deliberately offset blade, used to simulate fault conditions, is again clearly evident.
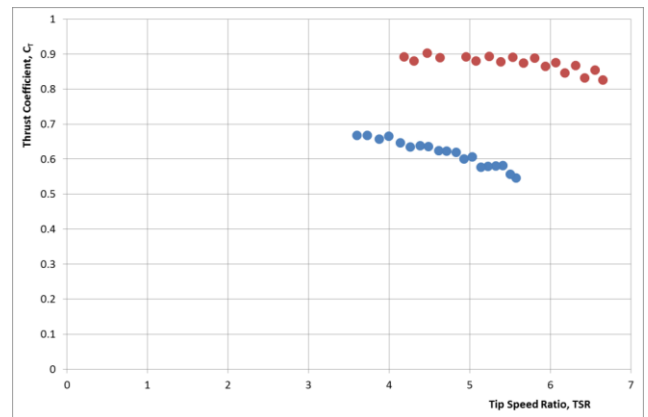

Fig. 5. Experimental Thrust Curves

The smaller cyclic variations in the larger overall axial thrust values that stem from blade-support structure interactions are shown in Fig. 6. This example result is for both optimum and offset blade cases, for 2 'mid-range' torque settings (30% and 32.5%) . The zoomed time axis is equivalent to approximately 5 turbine rotations for the conditions considered. These observations were the basis for instigating the time-frequency analyses.

The datasets from the legacy data acquisition system were not ideal for frequency domain analysis methods. The axial thrust was sampled at approximately 47.6 Hz. There was also evidence of quantisation effects in the digitized thrust signals [9]. For the 38 datasets the 90 s recordings represented between 192 and 359 turbine rotations, for angular velocities between 128 and 239 rev.min^{-1}. To progress, the analysis data from the entire duration were used in the frequency transforms. However, a simple statistical analysis revealed that for the optimum blade tests the typical angular velocity fluctuations were $\pm 2\%$ of mean values. For the offset blade test the fluctuations were generally larger and a typical value was $\pm 2.5\%$ of mean values [9].
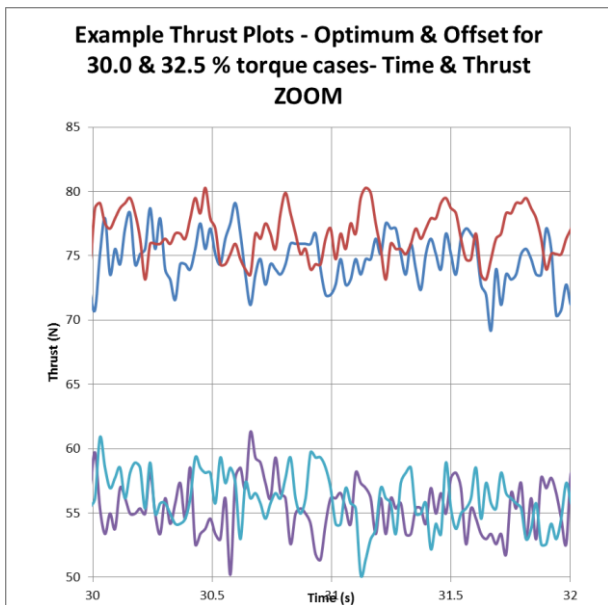
Fig. 6. Zoomed Axial Thrust and Angular Velocity Signals

Fig. 7. Spectrogram for Optimum Blades at 30% Torque

The 38 experimental datasets were initially analysed by using standard Fast Fourier Transform (FFT) functions with the Matlab environment. The obtained spectrums were investigated to determine whether differences between the optimum blade and offset blade subsets were reliably detectable. In all cases the rotational frequency (ω_r) was readily detectable, from the total axial thrust signals, and strongly correlated with the recorded angular velocities. Harmonics at $2.\omega_r$ and $3.\omega_r$ were generally detectable. The data limitations and the time varying turbine rotational velocities were deemed to reduce the clarity of such observations. Accordingly, time-frequency methods were employed. For the purpose of this summary, Fig. 7. shows a Matlab time-frequency plot. The spectrogram parameters, including the number of FFT points, the overlap extent and windowing, were optimized and the plots typically provided observable ω_r, $2.\omega_r$ and $3.\omega_r$ components. The example spectrogram plot in Fig.7. is for optimum blades at 30% torque. The 3 frequencies of interest are distinguishable, but not with sufficient resolution to determine their time variations.

A. Axial Thrust Parametric Modelling

The first stage in developing parametric models was to utilise more specific FSI simulation models. The parameters of the FSI models were configured in cognizance of the experimental axial thrust analyses. It was convenient to adapt existing FSI rotating blade models for a full size HATT. Fig. 8. shows the output for the 3 bladed 10 m diameter turbine, with the blades set at optimum pitch angles. Plug flow with a velocity of 3.086 ms^{-1} was used with operating conditions pertaining to a TSR of 3.61. For the full size turbine the latter equates to an angular velocity of 21.3 rev.min^{-1}.

The models are computationally intensive and settle to give steady state results. Fig. 8. shows the thrust components for 1 turbine revolution. As expected the blade effects, passing and shadowing the support tube, are offset by 120° from each other.
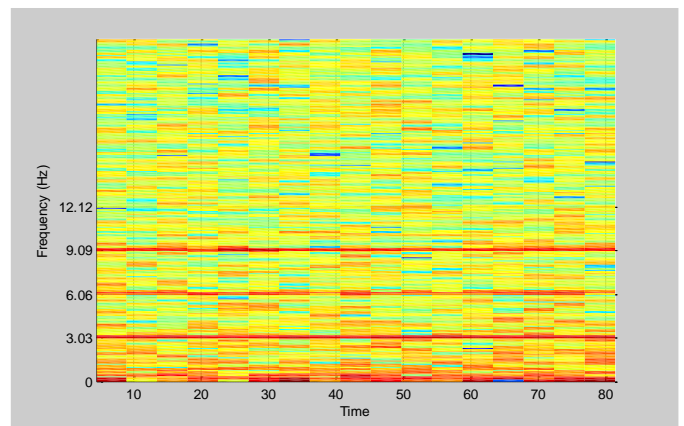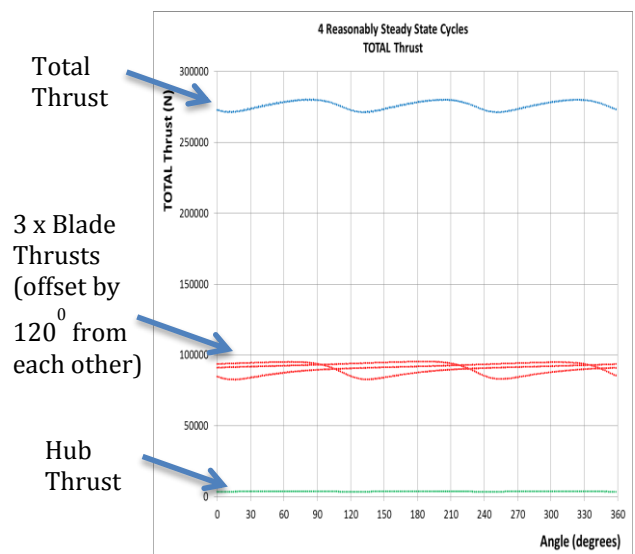

Fig. 8. CFD Modelling of Thrusts

Fig. 9. shows the thrust profile for 3 blades for 2 turbine revolutions. Fig. 9. also shows the frequency spectrum for an individual blade. The 8 constituent terms are all at multiples of the fundamental frequency and became the starting point for the parametric model. The average thrust value is not plotted. The FSI model assumes that the blades are identical and that all geometries are appropriately symmetrical. The individual blade results were combined to permit consideration and comparison of FFT spectrums for the total thrust cyclic variations.

It was found that tolerances pertaining to the experimental scale-size model needed to be considered. The manufacture of the turbine was to a high standard, however small eccentricity and other non-symmetries are likely. More particularly, the turbine was designed to have adjustable blade pitch angles. These were adjusted, and set as appropriate between tests, using a surface table and standard angle templates. There was some reliance on the skill and judgment of the experimenter. In contrast, the perfect symmetries and setups pertaining to the FSI models led to the observation that the frequency vectors from the 3 individual blades cancel each other out, except for those at $3.\omega_r$ and multiples thereof, when compiling the total axial thrust spectrums.
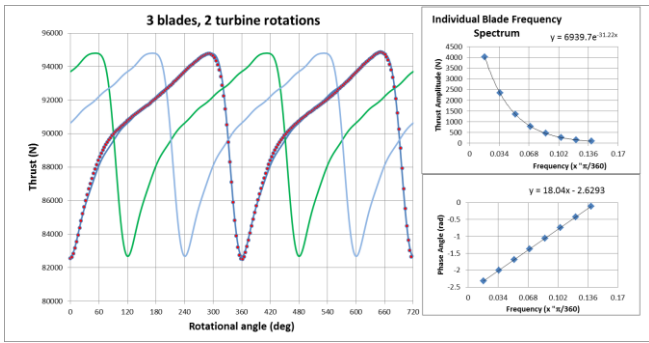
Fig. 9. CFM Model of Blade Thrusts and Individual Blade Frequency Spectrum.

Once relatively small adjustments were made, within the 8 term parametric model, then frequency components consistent to those in the experimental analysis were obtained. Fig. 10. shows FFT amplitude spectrum results when a 10% reduction in both the mean thrust and range of thrusts was applied for blade 2 only, with blades 1 and 3 retaining their optimum settings. The results then obtained for the total thrust are shown in Fig. 10.
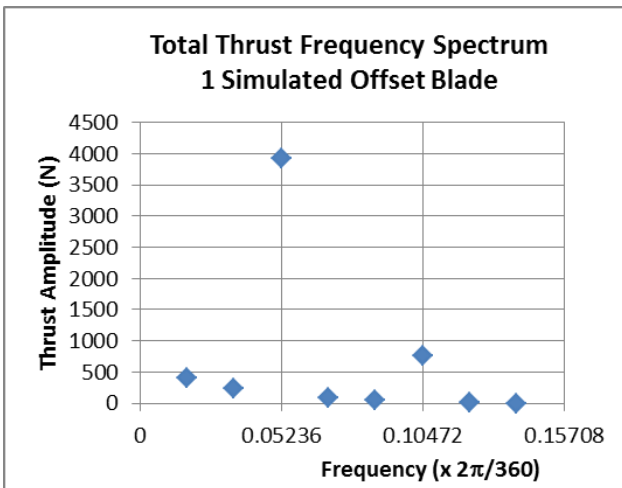

Fig. 10. Axial Thrust Amplitude Frequency Spectrum from 8-term parametric model with Simulated Effects due to Tolerances.

The adjustments were small compared to the difference in thrust values that would apply for the deliberately offset blade. For the offset blade the change to a 15° pitch angle is far more substantial, as previously discussed. Crucially, all ω_r, $2.\omega_r$ and $3.\omega_r$ components can be seen in the spectrum. The 8 term parametric model is orders of magnitude more computational time effective in comparison to the detailed FSI models.

V. DRIVE SHAFT TORQUE PARAMETRIC MODEL

A. Turbine Rotor Simulation Methodology.

Fig. 11. summarises the developed approach for generating synthetic driveshaft torque time-series. CFD simulations have been used to populate turbine performance curve information. The CFD and FSI simulations are used to determine the parametric model parameters to enable the evaluation of single blade fault conditions. The prior methods, described in section IV for axial thrust studies, were now applied to drive torque analysis. The characteristics, and in particular the periodic nature of, the

drive shaft torque fluctuations under various rotor conditions have accordingly been captured via a parametric model in the form of an 8 (or more) term Fourier series. The resource model is not detailed in this paper, but is used to allow realistic flow conditions and disturbances to be inputs to the parametric model. The output of the model are simulated rotor torques. These are available for time-frequency analysis and as drive signals for a motor-drive train- generator test rig.
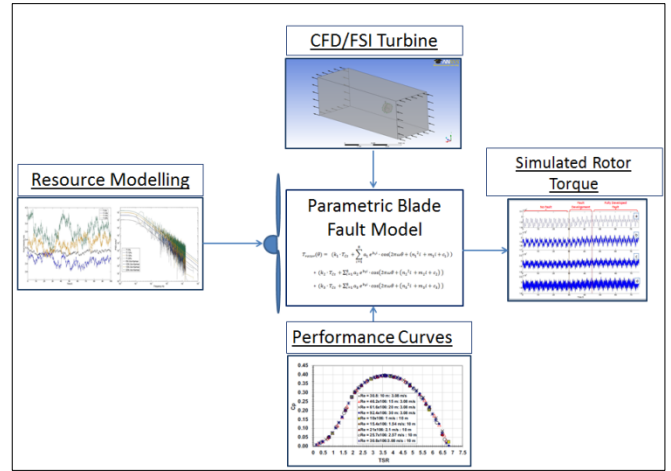

Fig. 11. Schematic representation of the simulation methodology

The parametric model was calibrated using the CFD model data and is calculated based on the parameter set associated with the rotor condition, the rotational displacement of the turbine and the characteristic or average fluid velocity over the turbine swept area. In order to impose a stochastic nature to the simulations the characteristic fluid velocity input into the parametric model has been modelled as stationary random process with a given power spectral density.

Fig. 12. further shows the contribution from experimental water flume testing of 0.5 m diameter scale-model turbines. Also shown is the motor-drive train- generator test rig. This is shown without any additional drive train components at this stage in the developing methods. It does facilitate the evaluation of generator outputs and their sensitivity to turbine blade faults. In simple terms recorded experimental data or other specific resource information may be used to drive the generator with realistic operating parameters. The parametric model can be configured to include blade faults, local turbulence / swirl and other flow conditions of interest.

In order to effectively simulate the resultant torsional load on the TST drive shaft computational fluid dynamic (CFD) modelling was used. CFD was utilised, as opposed to BEMT modelling with stochastic fluid field generation [13], as the resultant torque imposed on the drive shaft could be developed for a number of differing rotor conditions with a range of fluid flow complexities. The parametric model was constructed via a Fourier series evaluated at the turbine rotor position and could then be applied for differing rotor velocities by changing the frequency multiplier in each of the constituent terms.
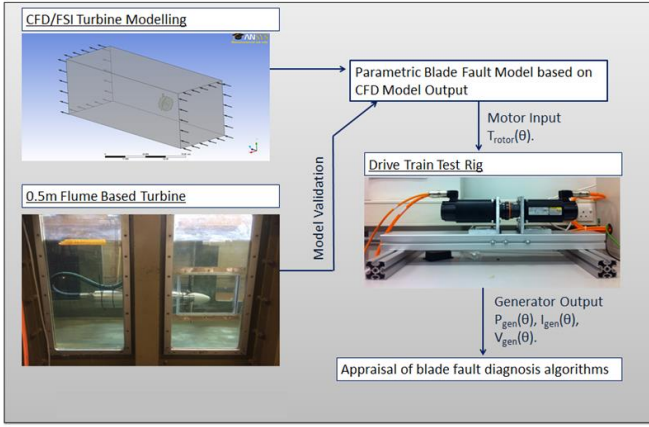
Fig. 12. Overview of CM testing methodology

A stochastic resource model was produced to simulate the turbulent flow structures in one dimension moving across the turbine. A number of simulations were produced for differing realisations of the resource model and for differing blade conditions.

B. TST Drive Train Emulator Test Rig.

Fig. 13. shows the motor-drive train-generator test rig developed for tidal stream turbine simulations. The test bed follows a similar structure to the one used by Yang et al [14] in that there is a motor controlled to replicate the turbine rotor input to the drive train. In this case the motor is directly coupled to a generator for power extraction thereby effectively simulating a direct drive turbine equipped with a permanent magnet synchronous generator (PMSG). To allow for flexibility during future testing the two rotating machines are mounted on slotted cross-sections allowing the separation between them to be increased so that gearboxes and other drive shaft components can be included in the test bed. The two rotating machines are of the servo type with on board encoders measuring the rotor velocity and position for feedback control. The machines are Bosch Rexroth IndraDyn MSK 050Cs and are synchronous permanent magnet machines rated with a maximum velocity of 4300 RPM and a maximum torque of 9 Nm. A Spiderflex rigid coupling is used to couple the machine's drive shafts.

The motor drive setup is shown in Fig. 14. The drives used are Bosch Rexroth IndraDrive Cs which, are set up as master and slave utilising the SERCOS III communication protocol. The master drive was then connected via Modbus TCP/IP to a National Instruments Compact RIO. The TST model and a maximum power point tracking control algorithm are implemented using the Real-Time operating system in the Compact RIO and the rotor and generator commands were sent to the motor drives via the Modbus link. The motor drives utilise close-loop current control to implement the commands sent from the Compact RIO. The drives implement field oriented control to set the torque on each machine to achieve the simulation commands at each time step - either drive shaft torque or rotational velocity. The parameters relating to both machines are sent to the Compact RIO for logging and further analysis.
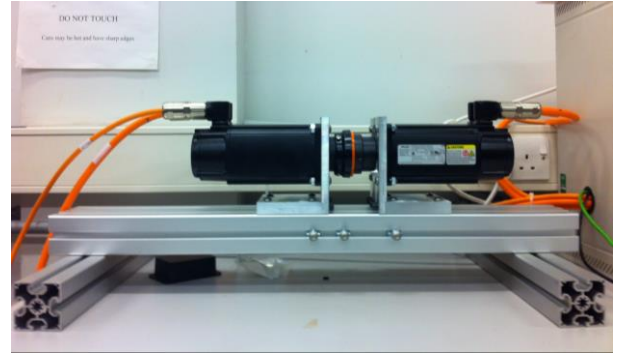

Fig. 13. TST Drive Train Test Rig Emulator.

Fig. 14. The motor drives coupled via SERCOS III connection with an NI CompactRIO for making calculations and sending drive commands.

C. Parametric Model.

The frequency content of the drive shaft torque calculated via CFD modelling was decomposed into the torque contribution by each turbine blade. Each blade exhibited relatively constant harmonic content at the rotational frequency of the turbine as well as the lowest seven harmonics of the rotational frequency of the turbine. Fig. 15. shows the angle-domain steady-state simulation results for the overall drive shaft torque.

The results for 2 revolutions show the constituent torques for the 3 identical and optimum pitch angle blades.

The frequency-domain spectrum is shown in Fig. 16. The consistent results for the optimum blades are shown in Fig. 16. along with the changes induced for 1 offset blade with increasing levels of offset. These levels are for blade pitch angles of 6.5º, 9º and 12º respectively. The parametric models, for a particular TSR, are detailed in Table 1.

TABLE1
TURBINE ROTOR TORQUE PARAMETRIC MODEL PARAMETERS AND VALUES

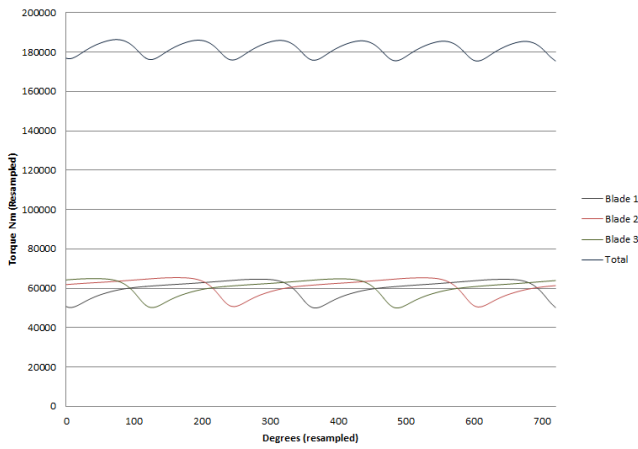|	Optimum			Offset 6.5			Offset 9			Offset 12		
Blade	1	2	3	1	2	3	1	2	3	1	2	3
K	0.310	0.313	0.310	0.327	0.318	0.316	0.344	0.314	0.298	0.337	0.309	0.285
A	8081	8442	8240	7741	8327	7843	9191	10354	9686	5387	8184	7820
B	-0.539	-0.551	-0.545	-0.552	-0.566	-0.552	-0.63	-0.616	-0.6	-0.519	-0.568	-0.56
M	-0.3696	-0.619	-0.529	0.3861	0.0026	-0.183	0.5875	0.6194	0.3209	0.1277	-0.119	-0.398
N	8.2552	9.7245	9.272	1.6031	3.8187	5.2636	-2.054	-2.351	-0.432	4.594	4.7638	6.7328
C	133.46	131.08	131.66	163.83	160.17	157.59	180.33	179.84	178.49	161.2	157.24	155.22
RMSE	0.0388	0.0858	0.0407	0.0799	0.0710	0.0811	0.0897	0.0701	0.0942	0.0942	0.0859	0.0974

Fig. 15. Resampled CFD results for two turbine rotation with optimum blade conditions showing the presence of the shadowing effect.
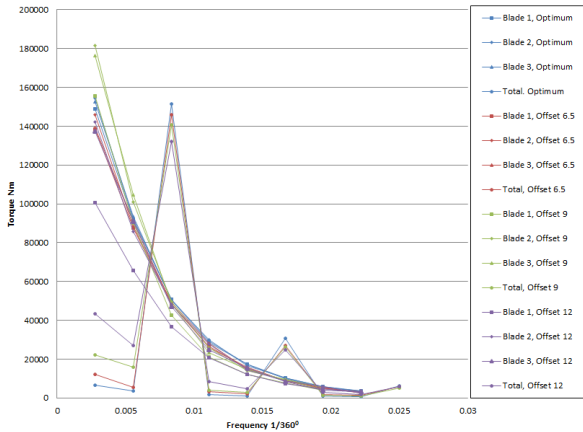

Fig. 16. Frequency spectrum of the CFD model torque output for differing rotor conditions showing 8 harmonic contributing to the overall drive shaft torque.

The drive torque parametric model was determined by turbine angular position, rather than being a time-based evaluation, and took a Fourier series of the form:

$$T_{rotor}(\theta) = \left(k_1 \cdot T_{Ct} + \sum_{i=1}^{8} a_1 \, e^{b_1 i} \cdot \cos\left(2\pi\omega\theta + \left(n_1^2 i + m_1 i + c_1\right)\right)\right)$$

$$+ \left(k_2 \cdot T_{Ct} + \sum_{i=1}^{8} a_2 \, e^{b_2 i} \cdot \cos\left(2\pi\omega\theta + \left(n_2^2 i + m_2 i + c_2\right)\right)\right)$$

$$+ \left(k_3 \cdot T_{Ct} + \sum_{i=1}^{8} a_3 \, e^{b_3 i} \cdot \cos\left(2\pi\omega\theta + \left(n_3^2 i + m_3 i + c_3\right)\right)\right).$$

In this investigation the focus was on TST operation at close to peak power conditions, rather than across the entire power curve. Accordingly, parameters where determined for tip speed ratios in the range 3.4 ± 0.2. The parameter values, as shown in Table 1 were sensibly constant over this range. This allowed parameters in the model to be held constant relative to the TSR. The parameter set was as follows:

K – Blade torque contribution for a given TSR
a – Depth of shadowing effect
b – Harmonic decay of the shadowing effect
n – Phase non-linearity
m – Phase gradient
c – Phase offset.

The parameter K gives the relative contribution of each blade to the total drive shaft torque; this in affect sets the DC value of the torque for a given TSR. The parameters a and b give the depth of the shadowing effect and the rate of decay of the 8 harmonics for each blade, this in effect defines the magnitude of torque fluctuations due to the aforementioned shadowing effect. Lastly, parameters m, n and c define the phase relationships over the 8 harmonics for each blade.

As stated previously, parameter sets were obtained for an optimum case (all blade pitch angles set to the 6°) and the three single-blade offset cases. Table 1 provides the parameter sets for a tip speed ratio of 3.4. The table also shows the RMSE between the model fit and the CFD data used to develop the model. A visual comparison of the parametric model and CFD simulations is provided in Fig.17.
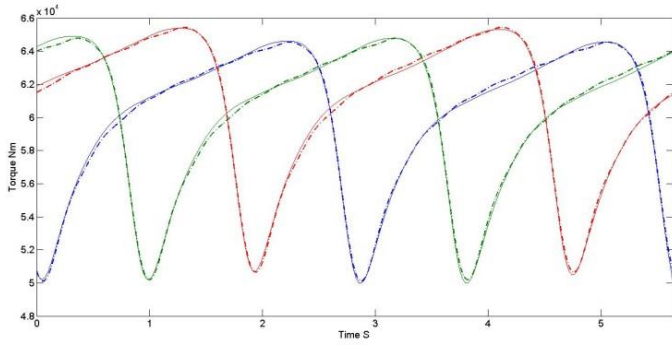
Fig. 17. Comparison of parametric model torque output with CFD model torque output.

D. Analysis of Parametric Model Outputs

The results presented in section VI were obtained via spectrogram and empirical mode decomposition methods.

The spectrogram results were produced using Matlab functionality. The spectrum analysis was conducted by appropriate setting of window length and overlap parameters in order to maximise the ability to identify anomalous rotor conditions deriving from blade fault conditions.

In general the envelope amplitude and the instantaneous frequency of a non-stationary signal will change over time. This leads to a significant problems for accurate estimation of the instantaneous frequency of a signal which can be of great interest in condition monitoring applications, such as torque signal analysis. However, it can be seen that for mono-component signals the instantaneous frequency can be estimated as the derivative of the signal phase relative to time . In order to exploit this, Hilbert-Huang transform techniques were evaluated. These techniques use Empirical Mode Decomposition (EMD)followed by construction of the Hilbert spectrum. Empirical mode decomposition represents the signal as a sum of Intrinsic Mode Functions (IMFs).

VI. RESULTS

Utilising the above simulation methodology a series of theoretical drive shaft torque time-series were generated for the appraisal of the time-frequency methods. The simulations were undertaken to appraise the effectiveness of the time-frequency analysis techniques for both differing turbulence intensities and differing turbine rotor conditions. In this manner the effectiveness of the algorithms for both detection and diagnosis could be gauged under varying sea conditions. For the study the simulations were conducted with the rotor condition set to optimum at the start of the simulation then the model parameters were changed after 30 seconds to simulate the onset of a turbine rotor fault. The fully developed fault was established over the subsequent 15 s period.

Fig. 18. is an example of the results obtained. The figure shows four developing scenarios for the 9° offset blade case, with the scenarios relating to increasing levels of turbulence being included in the model. The first case has no turbulent loading and the time series patterns correspond to the reported frequency content for the torque models. The other 3 cases have increasing

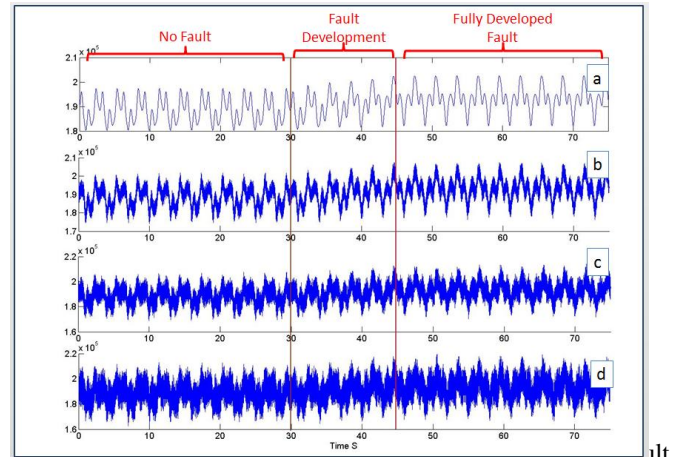turbulences, set at 0.05, 0.1 and 0.15 of the mean flow velocity respectively.

Fig. 17. Drive Shaft Torque Time Series with fault development and a) TI = 0, b) TI= 0.5, c) TI = 0.1 and d) TI = 0.15

The results of the spectrogram processing, for the same example case, are shown in Fig. 19. For clarity, the results for the 0.05 and 0.15 turbulences are shown as Figures (a) and (b) respectively with Fig. 19.
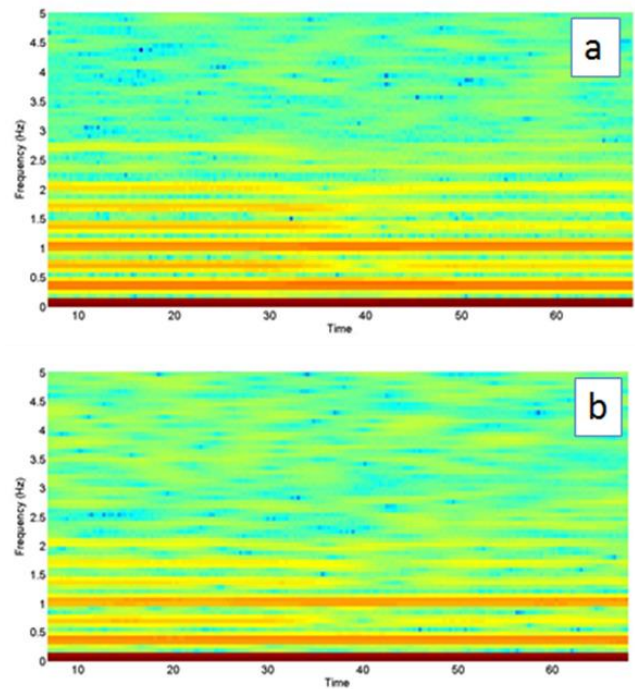

Fig. 19. Spectrogram of the drive shaft torque for a) TI = 0.05 and b) TI = 1.5

The spectrograms demonstrate that there are changes in the first 3 harmonics of the prevalent rotational frequency.

For the empirical mode decomposition method, the intrinsic mode functions are shown alongside time domain traces in Fig.20.. In this figure the results are shown for one of the scenarios, namely for a turbulence intensity setting of 0.05.
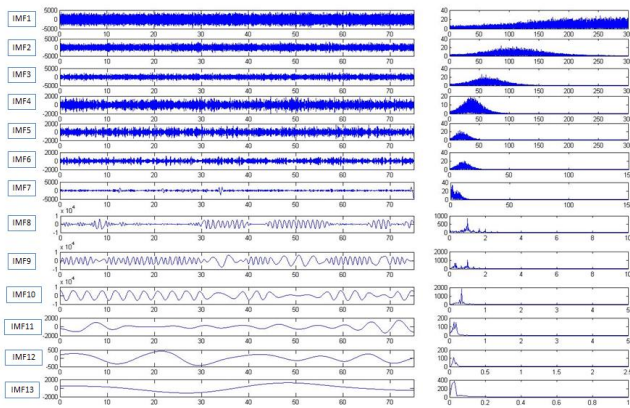
Fig. 20. Intrinsic mode functions for the drive shaft torque time series and the corresponding frequency spectrums.

VII. DISCUSSION

The techniques in use within CMERG aim to utilise the linkage between CFD/FSI simulations, the deployment and testing of scale-model TSTs and the signal acquisition and processing methods. For the development of condition monitoring systems for TSTs this is considered to be a useful framework for the evaluation of constituent monitoring systems.

This paper reports on experimental measurements of total axial thrust on a 3 bladed turbine. These derived from water flume tests at Liverpool University, who are partners in the same Supergen Marine consortium. The scale-model TST in use was the second within a generation of developing devices. Its primary function, when initially deployed, was the validation of simulation study results. Although the measured data was not ideal for time-frequency analysis it was sufficient to instigate such investigations. The TST shown in Fig. 12. is the next generation scale-model and has recently been deployed for testing. It has been designed with appropriate data acquisition, with significantly higher sample rates, and includes an instrumented hub. This allows an interface to blade torque sensors, 3-axis accelerometers and an encoder to synchronise the signals to turbine rotations.

The analysis of the axial thrust data led to the development of a per blade parametric model. As reported, the combination of 3 blades and the frequency spectrums obtained were investigated and compared to the experimental results. More specifically targeted simulations were also used to confirm the parameter values and their consistency.

Although developments have been made by Liverpool University to the water flume facility there are limits to the test configurations achievable. Their addition of a profiled flow setup and/or the addition of (axial direction) surface waves have enabled more comprehensive simulation validations.

The main benefits of the parametric modelling, particularly with its extension to the drive motor torques, are twofold. Firstly they are less time intensive, both in their configuration and in terms of the computation run-times. In combination with test beds, such as the motor-drive train-generator test rig, then realistic signals may be used to drive the motor such that it mimics turbine behaviour. The addition of other additional factors allows some evaluation of the robustness of proposed monitoring methods in the presence of swirl and turbulence, for example.

For the time-frequency examples reported it was observed that the spectrogram plots were generally unsuccessful in detecting the offset blade fault. There were, however some reductions observed for the higher frequency amplitudes, and that these effects were insensitive to the simulated level of turbulence intensity.

The empirical mode decomposition methods did provide good fault detection, with the intrinsic mode functions numbered IMF8 and IMF9 giving the most reliable detection for all tested turbulence intensity levels. The changes were detectable at relatively early stages of the deployed fault evolution test.

VIII. CONCLUSIONS

The potential use of drive shaft torques as a constituent within a TST condition monitoring system has been reported and discussed. This is considered to be an important parameter in both the condition monitoring and prognostics developments. The full-scale deployment of TSTs will inevitably mean that the operation and monitoring of each individual TST will be heavily site specific. The logging of operational conditions will be a vital element of the prognostic models. The recording and processing of the axial thrust signals will be another element with a role to play in such systems.

The parametric blade fault simulation model works adequately in simulating blade faults, with the prevalent plug flow conditions. This is typified by the small RSME values observed for the given test conditions.

The reported work is a contribution to the stated activities and will be extended with the aim of being even more complete and more able to mimic realistic flow conditions.

REFERENCES

[1] O'Doherty, T., Mason-Jones, A., O'Doherty, D.M., Evans, P.S., Woolridge, C.F. & Fryett, I. 'Considerations of a horizontal axis tidal turbine',*Energy,* vol 163 (issue EN3), pp119 – 130, 2010

[2] Mason-Jones, A., O'Doherty, D.M., Morris, C.E., O'Doherty, T., Byrne, C.B., Prickett, P.W., Grosvenor, R.I., Owen, I., Tedds, S. & Poole, R.J., Non-dimensional scaling of tidal stream turbines', *Energy,* vol 44, pp820 – 829,2012.

[3] Myers, L.E. & Bahaj, A.S., 'An experimental investigation simulating flow effects in first generation marine current energy converter arrays'**,** *Renewable Energy.* vol 37, pp 28 – 36, 2012.

[4] O'Doherty, D.M, Mason-Jones, A., O'Doherty, T., Byrne, C.B., Owen, I., & Wang, Y.X., 'Experimental and computational analysis of a model horizontal axis tidal turbine', *8th European Wave and Tidal Energy (EWTEC 2009).*

[5] Mason-Jones, A., O'Doherty, D.M., Morris, C.E., & O'Doherty, T. , 'Influence of a velocity profile & support structure on tidal stream turbine performance', *Renewable Energy.* Vol 52, pp 23 – 30. 2013.

[6] Grosvenor, R.I. & Prickett, P.W., 'A discussion of the prognostics and health management aspects of embedded condition monitoring systems', *Annual Conference of Prognostics and Health Management Society* 2011, 1 – 8, September 2011, Montreal.

[7] Bechhoefer, E., Wadham-Gagnon, M. & Boucher, B. *Annual Conference of Prognostics and Health Management Society* 2012, 1 – 8, September 23-27, Minneapolis.

[8] Uluyol, O. & Parthasarathy, G. *Annual Conference of Prognostics and Health Management Society* 2012, 1 – 8, September 23-27, Minneapolis.

[9] Grosvenor RI & Prickett PW, "The monitoring and validation of scale model tidal steam turbines", *Proceedings of Condition Monitoring and Diagnostic Engineering Management* , (2014) pp1-8.

[10] W. Yang, "Condition Monitoring the Drive Train of a Direct Drive Permanent Magnet Wind Turbine Using Generator Electrical Signals," *Journal of Solar Energy Engineering*, vol. 136, no. 2, p. 021008, 2014.

[11] W. Yang, P. J. Tavner, and R. Court, "An online technique for condition monitoring the induction generators used in wind and marine turbines," *Mechanical Systems and Signal Processing*, vol. 38, no. 1, pp. 103–112, Jul. 2013.

[12] Grosvenor RI, Prickett PW, Frost C, Allmark MJ, "Performance and condition monitoring of tidal stream turbines", *European Conference of Prognostics and Health Management Society 2014* , 1 (2014) 543-551 ISBN 9781936263165ISSN 2325-016X

[13] M. Togneri, I. Masters, J. Orme, and others, "Incorporating turbulent inflow conditions in a blade element momentum model of tidal stream turbines," *The Proceedings of the 21th*, 2011.

[14] W. Yang, P. J. Tavner, and M. Wilkinson, "Condition monitoring and fault diagnosis of a wind turbine with a synchronous generator using wavelet transforms," in *4th IET Conference on Power Electronics, Machines and Drives, 2008. PEMD 2008*, 2008, pp. 6 – 10.